

Penning trap mass measurements of $^{99-109}\text{Cd}$ with the ISOLTRAP mass spectrometer, and implications for the rp process

M. Breitenfeldt,^{1,*} G. Audi,² D. Beck,³ K. Blaum,^{4,5} S. George,^{4,6} F. Herfurth,³ A. Herlert,⁷ A. Kellerbauer,⁸ H.-J. Kluge,^{3,5} M. Kowalska,⁷ D. Lunney,² S. Naimi,² D. Neidherr,⁶ H. Schatz,^{9,10} S. Schwarz,⁹ and L. Schweikhard¹

¹*Institut für Physik, Ernst-Moritz-Arndt-Universität, D-17487 Greifswald, Germany*

²*CSNSM-IN2P3-CNRS, F-91405 Orsay-Campus, France*

³*GSI Helmholtzzentrum für Schwerionenforschung GmbH, Planckstraße 1, D-64291 Darmstadt, Germany*

⁴*Max-Planck-Institut für Kernphysik, D-69117 Heidelberg, Germany*

⁵*Ruprecht-Karls-Universität, Institut für Physik, D-69120 Heidelberg, Germany*

⁶*Institut für Physik, Johannes Gutenberg-Universität, D-55128 Mainz, Germany*

⁷*CERN, Physics Department, 1211 Geneva 23, Switzerland*

⁸*Commission of the European Communities, Joint Research Center, European Institute for Transuranium Elements, D-76125 Karlsruhe, Germany*

⁹*NSCL, Department of Physics and Astronomy, Michigan State University, East Lansing, Michigan 48824, USA*

¹⁰*Joint Institute for Nuclear Astrophysics, Michigan State University, East Lansing, Michigan 48824, USA*

(Received 17 April 2009; published 23 September 2009)

Penning trap mass measurements of neutron-deficient Cd isotopes $^{99-109}\text{Cd}$ have been performed with the ISOLTRAP mass spectrometer at ISOLDE/CERN, all with relative mass uncertainties below $3 \cdot 10^{-8}$. A new mass evaluation has been performed. The mass of ^{99}Cd has been determined for the first time, which extends the region of accurately known mass values toward the doubly magic nucleus ^{100}Sn . The implication of the results on the reaction path of the rp process in stellar x-ray bursts is discussed. In particular, the uncertainty of the abundance and the overproduction created by the rp -process for the mass $A = 99$ are demonstrated by reducing the uncertainty of the proton-separation energy of $^{100}\text{In } S_p(^{100}\text{In})$ by a factor of 2.5.

DOI: [10.1103/PhysRevC.80.035805](https://doi.org/10.1103/PhysRevC.80.035805)

PACS number(s): 21.10.Dr, 32.10.Bi, 26.30.Ca, 27.60.+j

I. INTRODUCTION

Penning ion traps are versatile tools used in many areas in atomic and nuclear physics. One application is high-precision mass spectrometry of atomic nuclei which leads to important input data for, e.g., nuclear structure studies [1,2]. Numerous results with very high precision have been reported from a number of facilities around the world for short-lived radioactive nuclides (ISOLTRAP [3], CPT [4], JYFLTRAP [5], LEBIT [6], SHIPTRAP [7], and TITAN [8]) covering the whole chart of nuclides. This allows one to test mass models and to improve mass predictions of exotic nuclides that have not been addressed so far. In nuclear astrophysics mass differences and thus nuclear masses are essential for the modeling of many nucleosynthesis sites. A current goal is the extension of high-precision mass measurements to nuclei very far from stability, in particular toward the very neutron-deficient nuclei in the rapid proton capture process (rp process) and toward the very neutron-rich nuclei in the rapid neutron capture process (r process). This goal is also addressed by storage ring mass spectrometry at the ESR facility at GSI [9]. ISOLTRAP has recently contributed a number of precision mass measurements to this area, such as ^{22}Mg [10,11] and ^{72}Kr [12,13] on the neutron-deficient

side and $^{80,81}\text{Zn}$ [14], ^{95}Kr [15], and $^{132,134}\text{Sn}$ [16,17] on the neutron-rich side.

In this article we present Penning trap mass measurements of neutron-deficient Cd isotopes out to ^{99}Cd that are important for modeling the isotopic abundances produced by the astrophysical rp process [18–21]. The rp process is a sequence of rapid proton captures and β^+ decays, often close to the proton drip line. For the $A \approx 99$ mass region, the rp process has been suggested [18,19] and discussed [22] as a candidate to explain the long-standing puzzle of the origin of the relatively large amounts of $^{92,94}\text{Mo}$ and $^{96,98}\text{Ru}$ in the solar system [23]. These form a lower-abundance group of so-called “ p nuclei” that are shielded from neutron capture in the s and r processes, which synthesize the rest of the heavy elements in nature. Whereas standard p -process scenarios based on photodisintegration processes produce most other p nuclei, they severely underproduce $^{92,94}\text{Mo}$ and $^{96,98}\text{Ru}$ [24,25].

The rp process is the main energy source of type I x-ray bursts on the surface of accreting neutron stars [26]. In some bursts characterized by long time scales of the order of 100 s, the rp process can reach the Cd region [27]. A reliable estimate of the produced composition is needed to model neutron star crust processes that are related to a number of observables, such as the rare superbursts or the cooling of transiently accreting neutron stars [28]. In addition, it has been shown that a small fraction of the processed matter could be ejected during x-ray bursts, renewing interest in these scenarios in terms of producing the Mo and Ru p isotopes [29].

*Corresponding address: CERN, Physics Department, 1211 Geneva 23, Switzerland; Martin.Breitenfeldt@cern.ch. This publication is part of the Ph.D. thesis of M. Breitenfeldt.

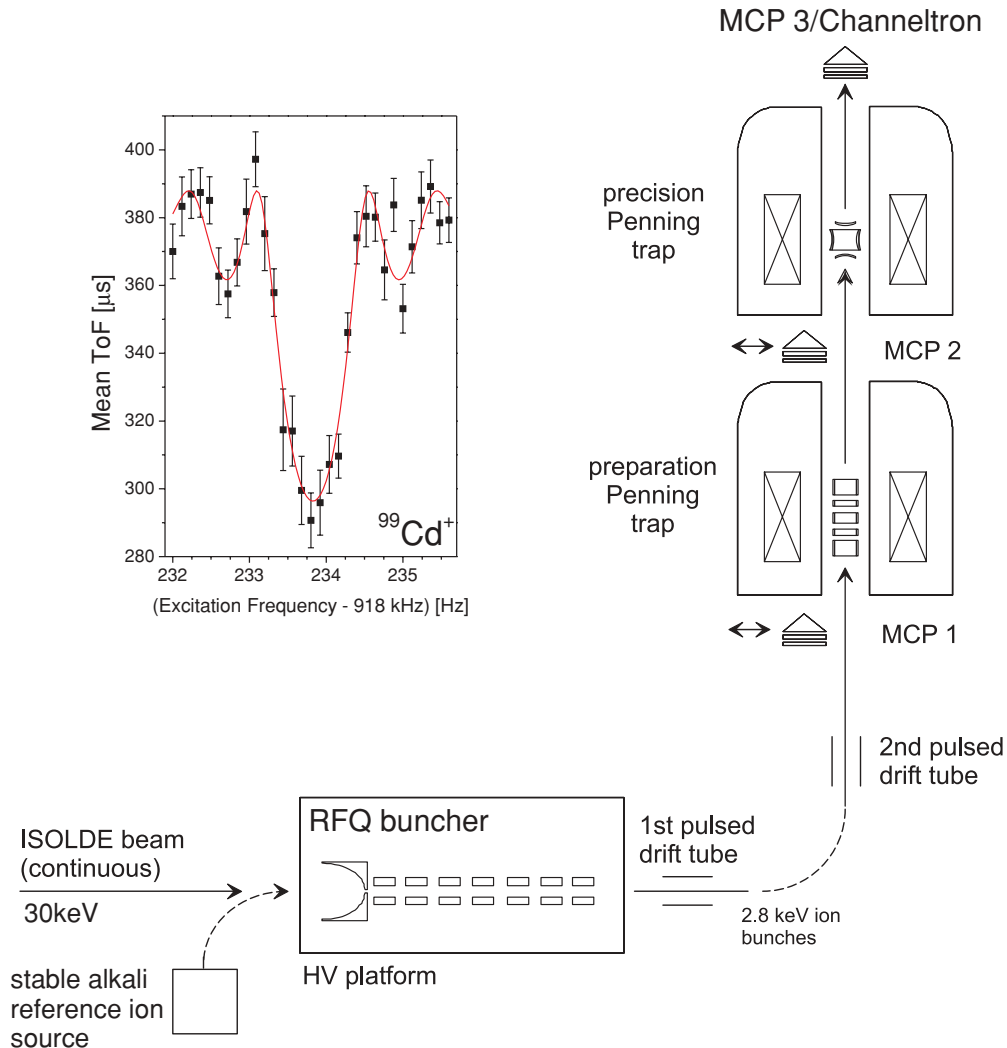


FIG. 1. (Color online) The triple-trap mass spectrometer ISOLTRAP with the three main parts: an RFQ buncher and two Penning traps. The inset shows a typical time-of-flight ion-cyclotron resonance for $^{99}\text{Cd}^+$ with a fit of the theoretical line shape (solid line) to the data [41].

The rp process is also thought to occur in proton-rich neutrino-driven outflows in core-collapse supernovae [20,21]. Because of the prominent role that neutrinos play in this nucleosynthesis it is referred to as “ νp process.” It has been shown that for certain model parameters the process can synthesize the Mo and Ru p isotopes and that it passes through the ^{99}Cd region investigated in this work [21]. For both scenarios the importance of accurate nuclear masses has been discussed before [21,22,30–33].

II. SETUP AND PROCEDURE

The measurements have been performed at the triple-trap mass spectrometer ISOLTRAP [3] at the isotope separator ISOLDE [34] at CERN, Geneva. As shown in Fig. 1, ISOLTRAP consists of three main parts: a linear radio frequency quadrupole (RFQ) buncher [35,36] for accumulation of the ions; a gas-filled cylindrical Penning trap for cooling, centering, and mass separation of the ions [37]; and a

hyperbolic Penning trap in an ultra-high vacuum for the determination of the cyclotron frequency ν_c . The present status of the experimental setup is described in more detail in Ref. [3].

In this work the Cd isotopes were created by 1.4-GeV proton pulses impinging on a Sn liquid-metal target with a thickness of 115 g cm^{-2} . After evaporation from the target the cadmium atoms were ionized in a FEBIAD hot plasma ion source [38], accelerated to 30 kV, sent through the general purpose separator (GPS) with a resolving power of $m/\Delta m = 800$, and transported to the ISOLTRAP experiment.

At ISOLTRAP the ions were accumulated and cooled in the RFQ buncher [36], which was elevated to a potential of 30 kV to decelerate the incoming continuous radioactive ion beam. The ions were ejected with a bunch length of about $1 \mu\text{s}$ and sent to the preparation Penning trap where the buffer-gas cooling technique [37] with a resolving power of about 20 000 was applied for isobaric purification. Figure 2 shows an example of a cooling resonance for $^{99}\text{Cd}^+$. The number of detected ions after centering is plotted as a function of the quadrupolar rf excitation frequency. The central

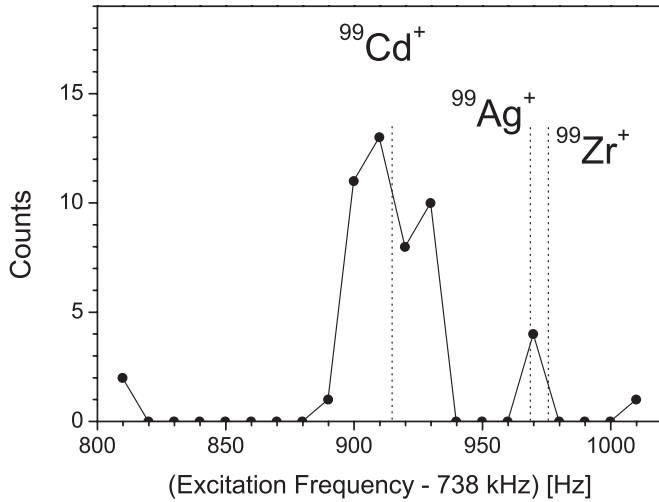


FIG. 2. A cooling resonance for $^{99}\text{Cd}^+$ in the preparation trap. The number of ions observed after ejection is plotted as a function of the excitation frequency ν_{rf} . $^{99}\text{Cd}^+$ is centered at about 738.92 kHz. Dashed lines indicate the positions of the cyclotron frequencies of $^{99}\text{Ag}^+$ and $^{99}\text{Zr}^+$, respectively.

peak corresponds to $^{99}\text{Cd}^+$, whereas the small peak to the higher-frequency side corresponds to the frequency of $^{99}\text{Ag}^+$. Note that $^{99}\text{Zr}^+$ would appear at almost the same cyclotron frequency as $^{99}\text{Ag}^+$, but is not expected to be released from the target. Subsequently the ions were transferred to the precision Penning trap for the determination of the cyclotron frequency ν_c using the time-of-flight ion-cyclotron-resonance (ToF-ICR) method [39,40]. The value for ν_c was obtained by fitting the theoretical line shape of the ToF-ICR to the data [41].

In the case of ^{103}Cd a possible ^{103}Mo contamination at $m/\Delta m = 480\,000$ was excluded by the application of a corresponding dipolar excitation at the reduced cyclotron frequency of the contaminant in the precision trap, which leads to radial ejection [42]. In all other cases the masses of possible contaminants are sufficiently far away from the masses of the nuclides of interest to eliminate them during cyclotron cooling in the preparation trap.

TABLE I. Half-lives and cyclotron frequency ratios $r = \nu_c(^{85}\text{Rb}^+)/\nu_c(^A\text{Cd}^+)$ between the reference nuclide ^{85}Rb and the neutron-deficient cadmium nuclides $^{99-109}\text{Cd}$.

Nuclide	Half-life	$r = \nu_c(^{85}\text{Rb}^+)/\nu_c(^A\text{Cd}^+)$
^{99}Cd	16(3) s	1.165 032 756 0(202)
^{100}Cd	49.1(0.5) s	1.176 755 855 2(208)
^{101}Cd	1.36(5) min	1.188 512 101 2(189)
^{102}Cd	5.5(0.5) min	1.200 240 767 7(218)
^{103}Cd	7.3(0.1) min	1.212 005 235 3(250)
^{104}Cd	57.7(1.0) min	1.223 740 297 6(228)
^{105}Cd	55.5(0.4) min	1.235 512 679 7(182)
^{106}Cd	Stable	1.247 254 328 2(215)
^{107}Cd	6.50(2) h	1.259 033 102 3(225)
^{108}Cd	Stable	1.270 781 503 2(270)
^{109}Cd	461.4(1.2) d	1.282 567 977 2(219)

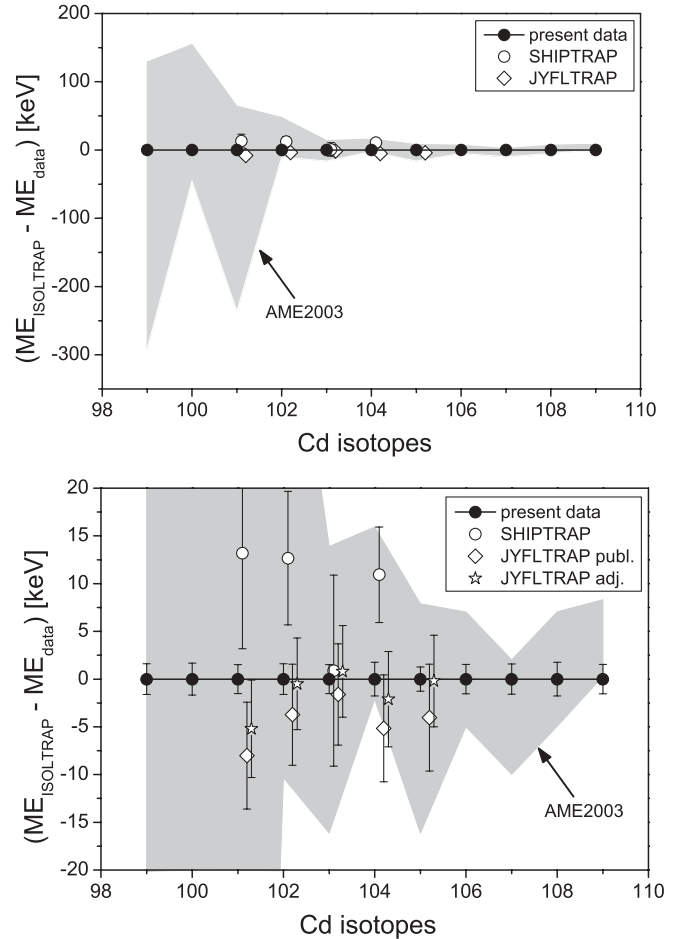


FIG. 3. (Top) Differences between the new mass-excess values measured at ISOLTRAP (solid circles) and those from AME2003 [46] and from SHIPTRAP [47] (open circles) and JYFLTRAP [48] (open squares). The new ISOLTRAP masses were chosen as a reference. The shaded area represents AME2003 values. (Bottom) Vertical zoom of top figure including recalculated values from JYFLTRAP using the mass of ^{96}Mo from the most recent AME (stars).

The measured cyclotron resonances were investigated with respect to possible shifts due to the presence of simultaneously stored isobaric ions by the standard analysis procedure applied at ISOLTRAP [3,43]. No indication for any contamination was found. This procedure has repeatedly demonstrated that uncertainties down to $2 \cdot 10^{-8}$ are possible and reproducible with ISOLTRAP [44,45].

III. EXPERIMENTAL RESULTS

Over a period of 5 days between three and five resonances for each of the 11 investigated nuclides $^{99-109}\text{Cd}$ were recorded. The inset of Fig. 1 shows a typical example for a ToF-ICR curve of $^{99}\text{Cd}^+$. The magnetic field strength is interpolated between two reference measurements of $^{85}\text{Rb}^+$. The averaged values of cyclotron frequency ratios r between the reference nuclide ^{85}Rb and the neutron-deficient Cd isotopes $^{99-109}\text{Cd}$, $r = \nu_c(^{85}\text{Rb}^+)/\nu_c(^A\text{Cd}^+)$, are given in Table I.

TABLE II. The mass excess (ME) of the neutron deficient Cd isotopes with $A = 99-109$ for the measurements performed at ISOLTRAP (this work), SHIPTRAP [47], and JYFLTRAP [48]. The adjusted JYFLTRAP ME values calculated from the frequency ratios published in Ref. [48] using a reference from the current AME are given in the last column.

Nuclide	ME(ISOLTRAP)/keV	ME(SHIPTRAP)/keV	ME(JYFLTRAP publ.)/keV	ME(JYFLTRAP adj.)/keV
⁹⁹ Cd	-69931.1(1.6)			
¹⁰⁰ Cd	-74194.6(1.6)			
¹⁰¹ Cd	-75836.4(1.5)	-75849(10)	-75827.8(5.6)	-75831.2(5.1)
¹⁰² Cd	-79659.6(1.7)	-79672(7)	-79655.6(5.3)	-79659.1(4.8)
¹⁰³ Cd	-80651.2(2.0)	-80651(10)	-80648.5(5.3)	-80652.0(4.8)
¹⁰⁴ Cd	-83968.5(1.8)	-83979(5)	-83962.9(5.6)	-83966.4(5.0)
¹⁰⁵ Cd	-84334.0(1.4)		-84330.1(5.5)	-84333.8(4.8)
¹⁰⁶ Cd	-87130.4(1.7)			
¹⁰⁷ Cd	-86990.4(1.8)			
¹⁰⁸ Cd	-89252.7(2.1)			
¹⁰⁹ Cd	-88503.7(1.7)			

As shown in Fig. 3, the measurements performed at ISOLTRAP (solid symbols) agree with the literature values of the latest Atomic-Mass Evaluation (AME2003) [46] within the uncertainties. Note that the mass of ⁹⁹Cd was determined experimentally for the first time. This plot also contains the recent mass-excess values obtained by SHIPTRAP at GSI [7] and by JYFLTRAP at IGISOL [5]. In these campaigns the masses of ¹⁰¹⁻¹⁰⁵Cd have been determined [47,48], as listed in Table II and plotted as open symbols in Fig. 3. In the case of the SHIPTRAP measurements a tendency to higher mass-excess values is observed. A new mass evaluation has been performed for this article to present the full impact of these and related results from the same region. The new evaluation follows exactly the same procedure as that outlined in the AME2003 [49], but using the updated flow-of-information matrices. A first evaluation was calculated including the values of SHIPTRAP and JYFLTRAP and a second was calculated including also ISOLTRAP. New averaged values were obtained, which are given in the last two columns of Table III and demonstrate the influence of the ISOLTRAP data.

IV. DISCUSSION

A. Mass evaluation

In the following the results obtained in this work are compared to previous data that were available for the atomic-mass evaluation in 2003 [46]. In Fig. 4 differences between mass-excess values obtained from ISOLTRAP and from the other two Penning trap experiments and the AME2003 are plotted as well as from mass-excess values calculated from the input data of the AME2003.

The SHIPTRAP data were already included in the mass evaluation, as published by Martín *et al.* [47]. The JYFLTRAP frequency ratios from Ref. [48] were included in the present evaluations as given in Table III in the last two columns. Using the ISOLTRAP frequency ratios a new atomic-mass evaluation was performed to check the influence of the new data on the AME network (Table III, last column). The individual cases are discussed in the following sections but there is an important general observation: Since the last published evaluation (in 2003 [46]), the masses of many nuclides have changed. One of these is ⁹⁶Mo, the reference mass used by

TABLE III. The mass excess (ME) of the neutron-deficient Cd isotopes with $A = 99-109$ for the measurements performed at ISOLTRAP (this work), those listed in the AME2003 [46], those obtained in an atomic-mass evaluation before the ISOLTRAP data entered (including SHIPTRAP [47] and JYFLTRAP data [48]), and the newly adjusted values (last column). The symbol # marks the AME value of ⁹⁹Cd as extrapolated from systematics.

Nuclide	ME(ISOLTRAP)/keV	ME(AME2003)/keV	ME(AME before)/keV	ME(AME after)/keV
⁹⁹ Cd	-69931.1(1.6)	-69850(210)#	-69850(210)#	-69931.1(1.6)
¹⁰⁰ Cd	-74194.6(1.6)	-74250(100)	-74252(65)	-74194.6(1.7)
¹⁰¹ Cd	-75836.4(1.5)	-75750(150)	-75835.8(4.8)	-75836.0(1.4)
¹⁰² Cd	-79659.6(1.7)	-79678(29)	-79664.4(4.1)	-79659.5(1.7)
¹⁰³ Cd	-80651.2(2.0)	-80649(15)	-80656.3(4.2)	-80652.0(1.8)
¹⁰⁴ Cd	-83968.5(1.8)	-83975(9)	-83968.7(4.7)	-83968.3(1.6)
¹⁰⁵ Cd	-84334.0(1.4)	-84330(12)	-84334.4(4.9)	-84333.8(1.3)
¹⁰⁶ Cd	-87130.4(1.7)	-87132(6)	-87128.2(5.0)	-87130.4(1.7)
¹⁰⁷ Cd	-86990.4(1.8)	-86985(6)	-86986.3(5.7)	-86990.1(1.7)
¹⁰⁸ Cd	-89252.7(2.1)	-89252(6)	-89251.9(5.5)	-89252.6(2.1)
¹⁰⁹ Cd	-88503.7(1.7)	-88508(4)	-88508.2(3.4)	-88504.7(1.6)

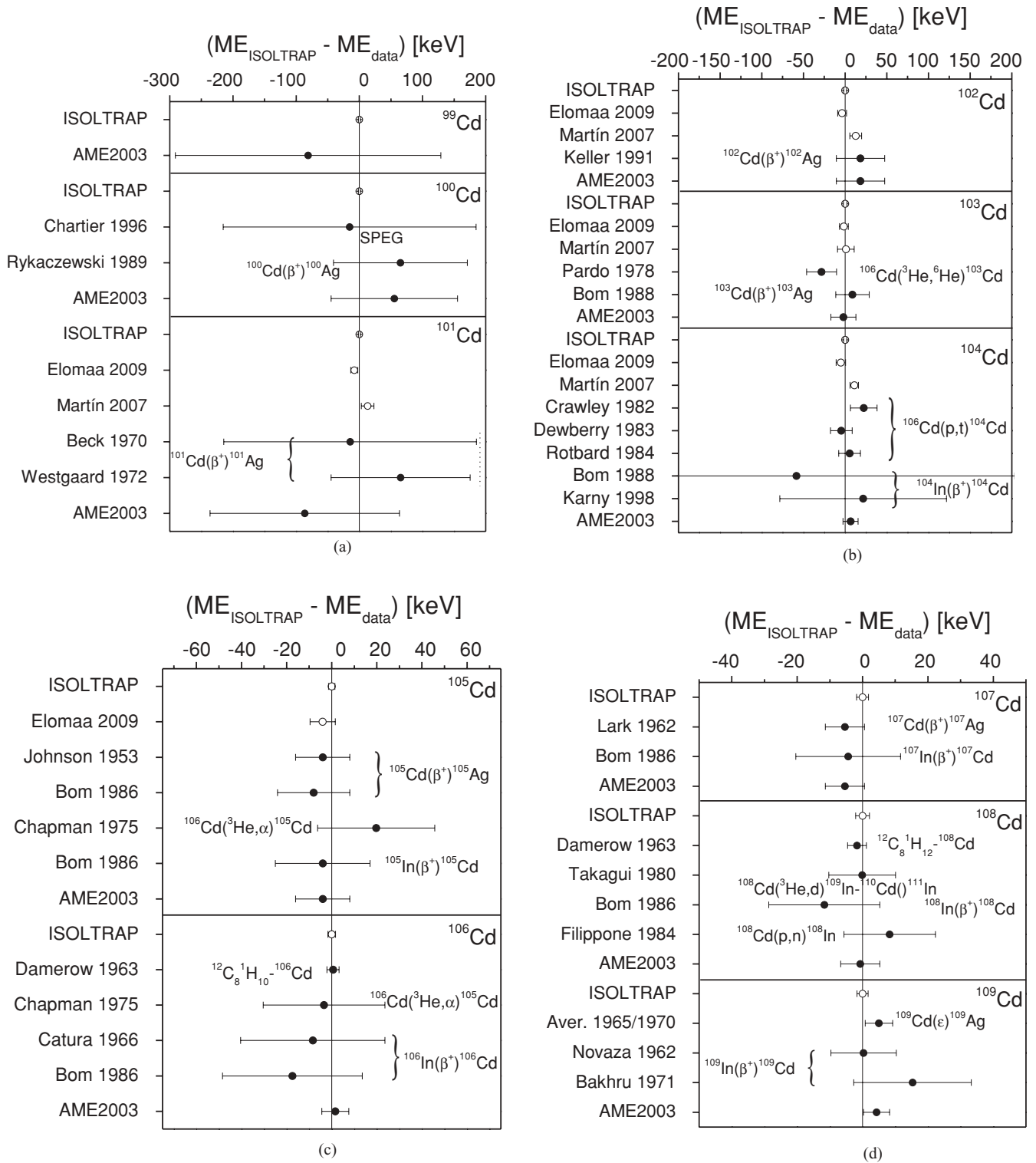


FIG. 4. Comparison of the mass-excess values of ISOLTRAP with the data of the Penning trap setups (SHIPTRAP [47], JYFLTRAP [48]), with the data that have been included in the AME2003 [46], and with the resulting AME2003 values for the nuclides $^{99}\text{--}^{109}\text{Cd}$. The braces connect similar reactions/experiments. The Penning trap values are marked with open circles; the older experimental data and the AME2003 values are indicated with solid circles.

JYFLTRAP to derive the masses in Ref. [48], which moved by 3.2 keV. Elomaa *et al.* [48] reported deviations of 1.8σ - 2.1σ from the SHIPTRAP mass values ($^{101,102,104}\text{Cd}$). When these masses are recalculated using the new ^{96}Mo mass value, the new JYFLTRAP values are in perfect agreement with those of ISOLTRAP and the deviation from the SHIPTRAP values is reduced to slightly over 1σ [see Fig. 3 (bottom) and Table II].

The reasons for the ^{96}Mo mass change are multiple, mostly related to the removal or replacement of conflicting data that were linked to ^{96}Mo (causing a -3.2 -keV shift between the AME2003 and the new AME). The question of links is a key point here. It is important to remember that it is not a mass that is measured in a trap, but rather a cyclotron frequency ratio, i.e., a link between two nuclides. As the reference a nuclide is chosen that already has a small uncertainty in its mass. In the case of ^{96}Mo , the uncertainty was 1.9 keV. Because JYFLTRAP reported several frequency ratios involving this nuclide, the ensemble of these links also contributed to a reduction in the ^{96}Mo uncertainty (to 1.5 keV) as well as the remaining 0.1 keV shift. Hence this is a case that illustrates the importance of the mass evaluation. For this reason the following discussion refers to JYFLTRAP data recalculated with the new ^{96}Mo mass instead of to the published values [48], to avoid conflicts, which are already solved in the present adjustment.

Like JYFLTRAP, the SHIPTRAP measurements contribute only slightly to the final mass results as compared to ISOLTRAP. In the AME, there is a distinction between “influence” (how much a datum affects a particular mass) and “significance” (how much a datum affects all the table). It is the policy of the AME that only data having a significance of more than one-ninth are used in the flow-of-information matrix [49]. This minimizes the propagation of inaccurate data with no sacrifice in overall precision.

The SHIPTRAP data [47], obtained by measuring the link ^{85}Rb - ^ACd , contribute less than the cutoff criterion for the case of the cadmium mass values as given in Table IV. Moreover, they have no influence on the value of ^{85}Rb as it was measured in Ref. [50] to an accuracy of about 11 eV. Thus, the significance of the SHIPTRAP data is concentrated on the mass being investigated. As a consequence, the SHIPTRAP data shown in Table II are excluded from the evaluation.

This is different for the data from JYFLTRAP. As can be seen from Table IV, the JYFLTRAP data have low influence on the cadmium mass values. However, JYFLTRAP has investigated the link ^{96}Mo - ^ACd . Because the mass value of ^{96}Mo was previously known only to 1.9 keV, there is also a flow of information from the JYFLTRAP data toward ^{96}Mo . The “influence” of the JYFLTRAP data reduces the uncertainty of the ^{96}Mo mass value to 1.5 keV as shown in Fig. 5 and therefore the “significance” of the JYFLTRAP data is increased. Therefore these data are included in the evaluation.

The comparison of the input data to the new AME value is shown in Fig. 6. Note that due to feedback from the new data the plotted mass-excess values can shift as compared to Fig. 4.

TABLE IV. The influences of the experimental data from ISOLTRAP (this work) and from JYFLTRAP [48] on the current AME on the mass-excess values of ^ACd and ^{96}Mo . The given influences of the SHIPTRAP data [47] are hypothetical; these data have not been included because of their low significance.

Nuclide	Influences of experimental data			
	On the Cd nuclides			On ^{96}Mo
	ISOLTRAP	SHIPTRAP ^a	JYFLTRAP	JYFLTRAP
^{99}Cd	100%			
^{100}Cd	100%			
^{101}Cd	92.9%	2% ^a	7.1%	9.0%
^{102}Cd	89.4%	6% ^a	10.6%	9.9%
^{103}Cd	84.7%	3% ^a	12.3%	9.9%
^{104}Cd	90.3%	10% ^a	9.7%	9.3%
^{105}Cd	92.9%		6.4%	10.2%
^{106}Cd	99.7%			
^{107}Cd	91.5%			
^{108}Cd	94.0%			
^{109}Cd	82.9%			

^aHypothetically.

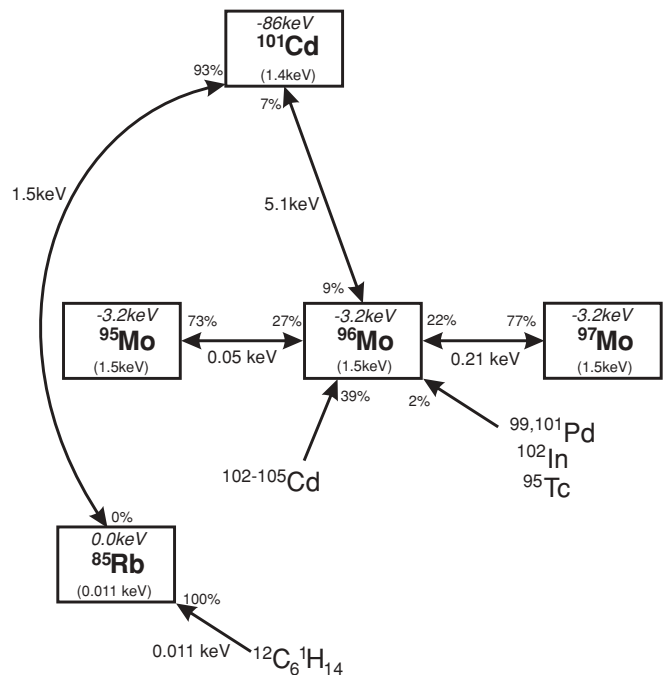


FIG. 5. A zoom into the network of experimental results and mass values on the nuclides ^{101}Cd and ^{96}Mo for the current evaluation. The boxes represent nuclides with their uncertainties. The *italic* numbers indicate the shift of the mass-excess value as compared to the AME2003. The connections between the boxes with the arrowheads show the influences of the data on the corresponding masses. The values close to the links represent the uncertainties of the data. In the case of frequency ratios the experimental results are linearized, to do matrix calculations [46]. The data with low influence on ^{96}Mo connecting to $^{99,101}\text{Pd}$, ^{102}In , and ^{95}Tc are mainly determining the other end of the link and thus are above the limit for insignificance.

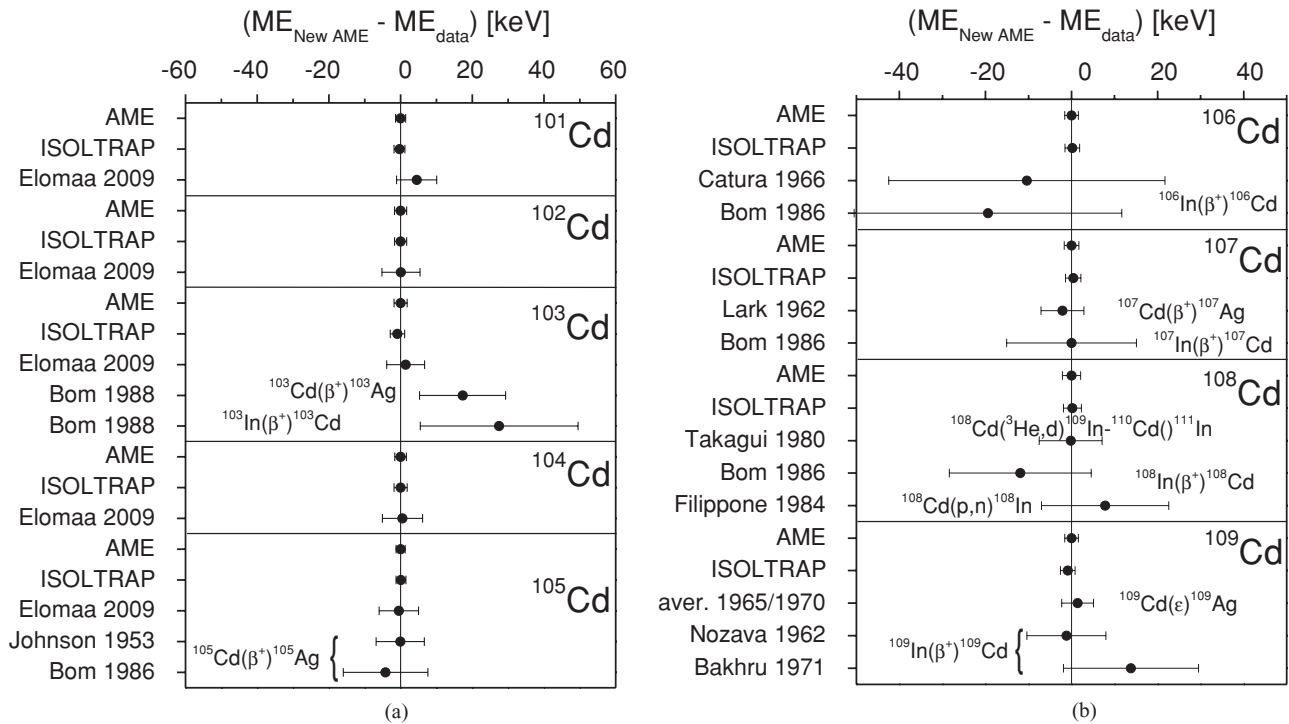


FIG. 6. The difference of the contributing experimental data to the newly evaluated atomic-mass excess is plotted. Note, that the input values might have changed slightly because of feedback from the data of this work. The braces connect the same reaction/experiment.

1. ^{109}Cd

The main contribution for the mass-excess value of the AME2003 came from an electron-capture measurement of ^{109}Cd to ^{109}Ag with a Q value of 214(3) keV as an average of two experiments [51,52] (84.7%). The other 15.3% was given by two β^+ -decay Q -value measurements, $Q = 2015(8)$ keV and $2030(15)$ keV [53,54]. The ISOLTRAP measurement agrees with the earlier values and decreases the experimental uncertainty. After a new evaluation the AME value is now influenced 82.9% by the ISOLTRAP data, 13.7% by the electron capture $^{109}\text{Cd}(e^-)^{109}\text{Ag}$ [51,52], and 3.5% by β^+ decay of the ^{109}In [53,54].

2. ^{108}Cd

The mass-excess value of ^{108}Cd in the AME2003 is calculated including an experimental value from the Minnesota, 16-inch, double-focusing mass spectrometer, namely the difference of $m(\text{C}_8\text{H}_{12}-^{108}\text{Cd}) = 189715.6(2.9) \mu\text{u}$ [55] with 67.9% influence and the Q value of the differential reaction of $^{108}\text{Cd}(^3\text{He},d)^{109}\text{In}-^{110}\text{Cd}(^111\text{In})$, $Q_0 = -806.5(2.6)$ keV [56] (27.1%). A small contribution comes from the average of a β^+ -decay Q value of ^{108}In [57] $Q = 5125(14)$ keV and the $^{108}\text{Cd}(p,n)^{108}\text{In}$ reaction [58] with a weight of 5.0%. The ISOLTRAP value compares to the AME2003 value within the uncertainties. The result of a new calculation of the AME is determined to 94.0% by the ISOLTRAP value with a three times smaller uncertainty. The value of the differential reaction [56] contributes 5.7% and the average of the β decay and the (p,n) reaction 0.3%.

3. ^{107}Cd

The mass excess of ^{107}Cd was determined by the Q -value measurements of two β^+ decays: $Q(^{107}\text{Cd}(\beta^+)^{107}\text{Ag}) = 1417(4)$ keV [59] and $Q(^{107}\text{In}(\beta^+)^{107}\text{Cd}) = 3426(11)$ keV [57], which entered with 96.3% and 3.7%, respectively, to calculate the AME2003 mass excess. This value agrees with the one from the present work. After reevaluating all data the new AME value is determined to 91.5% by the ISOLTRAP data. The rest is coming from the β^+ -decay Q values of $^{107}\text{Cd}(\beta^+)^{107}\text{Ag}$ [59] and $^{107}\text{In}(\beta^+)^{107}\text{Cd}$ [57] with 8.2% and 0.3%, respectively.

4. ^{106}Cd

The mass of ^{106}Cd was determined by the mass doublet of $\text{C}_8\text{H}_{10}-^{106}\text{Cd}$ and has been measured to $171\,789.3(2.7) \mu\text{u}$ [55] contributing to the average value in the AME2003 with 89.0%. Also the single-neutron pickup reaction $^{106}\text{Cd}(^3\text{He},\alpha)^{105}\text{Cd}$ [$Q_0 = 9728(25)$ keV] [60] enters with 4.4%, and the β^+ decay of ^{106}In with $Q = 6516(30)$ keV [61] and $Q = 6507(29)$ keV [57] combined with the $^{106}\text{Cd}(p,n)^{106}\text{In}$ reaction having a reaction Q value of $-7312.9(15.0)$ keV [58] contribute 3.5% to the mass-excess value of ^{106}Cd as tabulated in the AME2003. The measurement at ISOLTRAP agrees with these previous results, but has a four times smaller uncertainty. The new AME result has a 99.7% influence from the ISOLTRAP data. The β^+ decay of ^{106}In [57,61] and the (p,n) reaction [58] contribute only 0.3%. They have been included because of their significance as links in the mass network.

5. ^{105}Cd

The two direct mass measurements with the mass-excess values of JYFLTRAP and ISOLTRAP agree perfectly within their uncertainties. The previous mass-excess value tabulated in the AME2003 (including experimental data by Refs. [57,60,62]) is also in agreement within the uncertainties. The new AME value is determined to 92.9% by ISOLTRAP and to 6.4% by JYFLTRAP. The β^+ decay of ^{105}Cd [57,62] contributes with 0.7% the mass excess of ^{105}Cd . In addition, the sevenfold reduction of the uncertainty of ^{105}Cd mass results also in an improvement of the ME of ^{105}Ag by a factor of more than two to $-87\,070.8(4.5)$ keV.

6. ^{104}Cd

For $A = 104$ the results of ISOLTRAP and JYFLTRAP agree within the experimental uncertainties, while the SHIPTRAP result deviates from the ISOLTRAP and the JYFL-TRAP value by about 11 keV (2σ) and 12 keV (1.7σ), respectively. All values agree perfectly with the AME2003, which includes experimental data from Refs. [63–67], while reducing the uncertainty. The newly obtained AME value is 90.3% determined by the ISOLTRAP value and 9.7% determined by the JYFLTRAP result.

7. ^{103}Cd

In this case all three Penning trap measurements agree nicely with each other. Furthermore the three measurements are within the uncertainty of the AME2003 value, which includes experimental data from Refs. [66,68]. The newly determined AME value is influenced by 84.7% and 12.3% by the ISOLTRAP and the JYFLTRAP value, respectively. There are small contributions coming from the β decays $^{103}\text{Cd}(\beta)^{103}\text{Ag}$ (2.4%) and $^{103}\text{In}(\beta)^{103}\text{Cd}$ (0.6%).

8. ^{102}Cd

For this nuclide the mass excess also has been determined at SHIPTRAP and at JYFLTRAP. The two values have a discrepancy of 12 keV corresponding to 1.4σ . The ISOLTRAP value agrees well with the measurements at JYFLTRAP but deviates by 1.8σ from the values determined at SHIPTRAP. Also in this case all three Penning trap measurements agree with the mass excess listed in the AME2003, which includes experimental data from Ref. [69]. In the new compilation of the mass values for the AME, the ISOLTRAP result contributes 89.4% and the JYFLTRAP value contributes 10.6%.

9. ^{101}Cd

The mass excess of ^{101}Cd has been determined at SHIPTRAP and JYFLTRAP. Both values have a discrepancy of 1.5σ relative to each other. The mass excess determined at ISOLTRAP is between the two earlier results and deviates by 14 keV (1.3σ) from the SHIPTRAP results and agrees within the uncertainty with the result from JYFLTRAP. All three

values agree with the AME2003 mass excess determined in Refs. [70,71]. The new AME value is influenced 92.9% by the ISOLTRAP result and 7.1% by the JYFLTRAP result.

10. ^{100}Cd

So far, the mass excess of ^{100}Cd was determined using the SPEG mass spectrometer value of $-74\,180(200)$ keV [72] and via the Q value of the β^+ decay of ^{100}Cd to ^{100}Ag of 3890 keV [73]. The experimental result obtained at ISOLTRAP agrees very nicely with the earlier experiments, but the uncertainty is by more than a factor of 50 smaller. The new AME uses the ISOLTRAP data with 100% of influence for the determination of the ME of ^{100}Cd , and the connection by $^{100}\text{Cd}(\beta^+)^{100}\text{In}$ changes the mass excess of ^{100}In to a value of $-64\,330(180)$ keV, indicating that this nucleus is by 35 keV less bound as compared to the AME2003.

11. ^{99}Cd

The mass of ^{99}Cd was determined for the first time by ISOLTRAP. Before, only an AME2003 estimate of the mass excess was available, which agrees with the new value determined by ISOLTRAP.

B. Implications for the astrophysical rp process

^{99}Cd has been suggested as a possible branching point in the path of the astrophysical rp process in some x-ray bursts. Figure 7 shows the reaction flows during a type I x-ray burst calculated in a model based on a single-zone approximation and for parameters (accretion rate and initial composition) that are favorable for an extended rp process into the Sn region [27,74]. Here we updated the reaction network [75] with results from recent Penning trap mass measurements (by, e.g., LEBIT [76], CPT [22], JYFLTRAP [32,77], and SHIPTRAP [32,47]) and the new masses from this work.

Figure 7 shows the reaction paths for the entire burst. During the very end of the burst, as hydrogen abundance and temperature are dropping, the reaction path shifts toward ^{99}Cd (see Fig. 8). The amount of ^{99}Cd that can be built up by feeding from $^{98}\text{Cd}(\beta^+)^{98}\text{Ag}(p,\gamma)^{99}\text{Cd}$ depends critically on the remaining decrease of ^{99}Cd by proton captures before hydrogen is completely exhausted and the final abundances freeze out. This depends strongly on the proton-separation energy of ^{100}In , $S_p(^{100}\text{In})$. If this quantity is low, proton captures are inhibited by photodisintegration of ^{100}In , and ^{99}Cd remains abundant as the reaction flow proceeds via its slow β^+ decay. If $S_p(^{100}\text{In})$ is large, ^{99}Cd can be converted very effectively by a dominating reaction flow via $^{99}\text{Cd}(p,\gamma)^{100}\text{In}$.

The AME2003 value for $S_p(^{100}\text{In})$ is 1.61(33) MeV as obtained by adding mass errors quadratically. The large error originated from the extrapolated masses of ^{99}Cd (± 0.21 MeV) and ^{100}In (± 0.25 MeV). After our accurate measurement of the ^{99}Cd mass the uncertainty is almost exclusively due to the ^{100}In mass. Including the newly evaluated value for the mass of ^{100}In we obtain now $S_p(^{100}\text{In})$ of 1.69(18) MeV.

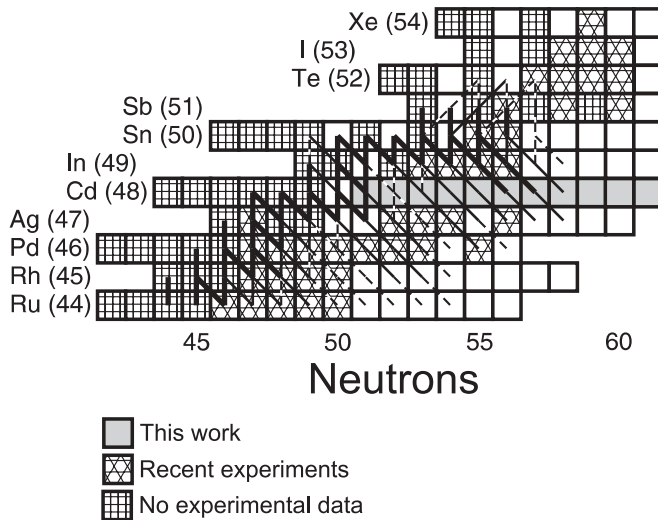


FIG. 7. A plot of the time integrated net reaction flows over the entire x-ray burst in the region of the nuclide chart around ^{99}Cd . The thick lines represent a strong flow (within an order of magnitude of the 3α reaction) and the thin and dashed lines represent weak flows suppressed by factors of 10 and 100, respectively. Note that strong proton capture flows either indicate strong net flows or, because of numerical artifacts, (p,γ) - (γ,p) equilibrium. The gray shaded nuclides were measured in this work, perpendicularly meshed nuclides represent extrapolated values [46], and the diagonally meshed boxes indicate nuclides recently measured in other experiments [22,32,47,77].

Figure 9 shows final abundances and overproduction factors relative to solar abundances for model calculations for various values of $S_p(^{100}\text{In})$. Clearly, $S_p(^{100}\text{In})$ is a critical quantity for determining the $A = 99$ abundance in the final reaction products (burst ashes). The 2σ range of the AME2003 mass uncertainties introduces more than an order of magnitude uncertainty in the $A = 99$ abundance. At the lower 2σ limit of $S_p(^{100}\text{In})$, $A = 99$ becomes one of the most abundant mass chains, even exceeding the $A = 98$ production by 50%, whereas at the upper limit it is one of the least abundant ones. Our new measurements dramatically reduce the possible range

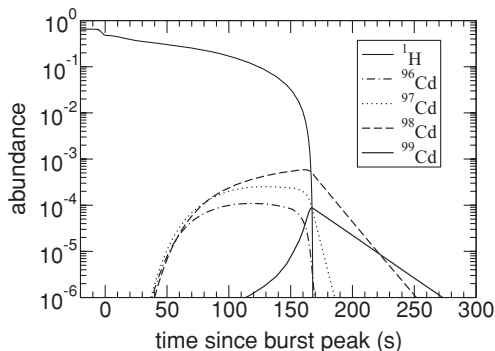


FIG. 8. Abundances of hydrogen and the neutron-deficient Cd isotopes as functions of time during an x-ray burst. Zero on the time axis has been chosen to coincide with the burst maximum. The buildup of Cd isotopes occurs during the tail of the burst.

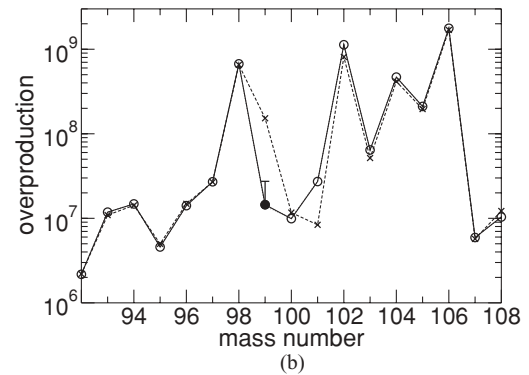
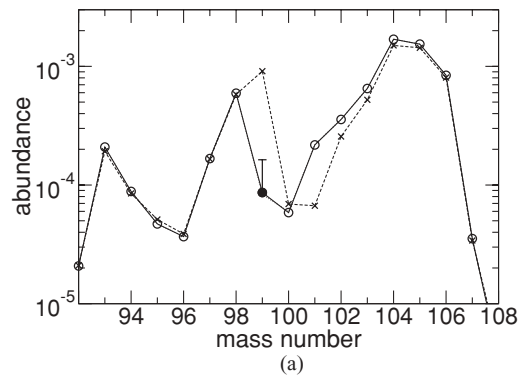


FIG. 9. (Top) Final composition of the burst ashes for different values of $S_p(^{100}\text{In})$: with our new value for ^{99}Cd (circles connected by solid line), the lower 2σ limit allowed in AME2003 (crosses connected by dashed line), and the upper 2σ limit allowed in AME2003 (dotted line that basically coincides with solid line). The data point with our new ^{99}Cd mass and our new 2σ uncertainty is indicated as a solid circle with error bars. (Bottom) Overproduction factors relative to the solar abundance, determined by assuming the entire mass chain has decayed into the first stable isotope. This is a p nucleus for $A = 92, 94, 96, 98, 102, 106$, whereas the other mass chains feed isotopes predominantly made by the s process.

of $A = 99$, excluding now an enhanced $A = 99$ production at the 2σ level. The largest reduction in the uncertainty comes from our precise measurement of the ^{99}Cd mass. However, the improvement in precision of the mass of ^{100}In due to the β^+ decay of ^{100}In linked to ^{100}Cd (measured in this work) contributes significantly, leading to an additional reduction of the uncertainty by about a factor of 2.5.

The composition of the burst ashes is important for crust heating models and for judging whether the rp process is a possible production scenario for light p nuclei. In terms of crustal heating, Gupta *et al.* [28] have shown that there are significant differences in total heat generation and distribution of heat sources as a function of depth for $A = 98, 99$, or 100 ashes. While a change in a single mass chain probably has only a small effect on the thermal structure of the neutron star, our work shows that there are very large uncertainties in the prediction of the final composition of the burst ashes that need to be addressed. Our measurement is a first step in that direction. Uncertainties in other mass chains will also have to be addressed.

To judge the suitability of a proposed nucleosynthesis scenario to explain the origin of the elements in the solar system, one key aspect is the pattern of overproduction factors, i.e., the ratio of the produced abundances to the solar abundances (see Fig. 9). The ratio of the overproduction factor of a given isotope to the highest overproduction factor of the pattern (or to an average of the highest overproduction factors when taking into account variations due to uncertainties) indicates the fraction of solar system material that could originate at most from this nucleosynthesis site. For a p -process scenario one would require large, comparable overproduction factors for p nuclei and significantly reduced overproduction factors for non- p nuclei. As Fig. 9 shows, the rp process in this particular x-ray burst would be a promising scenario to produce the p -nuclei ^{98}Ru , ^{102}Pd , and ^{106}Cd . However, coproduction of non- p nuclei such as isotopes fed by the $A = 99$, 104, and 105 mass chains potentially limits this scenario. The question is whether a possible coproduction can be attributed to uncertainties in the nuclear physics or whether it is a fundamental issue with the proposed scenario. For the $A = 99$ case, we have now addressed this question with the present measurement. As Fig. 9 shows, at the 2σ level the AME2003 mass uncertainties allowed for coproduction of as much as 20% of ^{99}Ru (an s -process nucleus) relative to the p -nucleus ^{98}Ru . With our new mass measurements, $A = 99$ coproduction is now limited to a rather insignificant few percent.

V. CONCLUSION AND OUTLOOK

In the present work, mass determinations of the eleven neutron-deficient nuclides $^{99-109}\text{Cd}$ are reported. Because of clean production of these nuclides it was possible to reduce the experimental uncertainties down to 2 keV. In the case of ^{99}Cd the mass was determined for the first time and for the nuclide ^{100}Cd the uncertainty was reduced by a factor of more than 50. In addition, the influence of the present results on the mass network of the atomic-mass evaluation is described as well as the role of the evaluation for solving conflicts of mass data like in the case of $^{101-105}\text{Cd}$ measured at ISOLTRAP, SHIPTRAP, and JYFLTRAP.

The presented mass measurements are an important step toward an understanding of the nuclear physics of the rp process that will enable a more reliable determination of the

composition of the produced material at $A = 99$. It was shown that the mass of ^{99}Cd strongly affects the $A = 99$ production in an x-ray burst model and that uncertainties have been significantly reduced from more than an order of magnitude to less than a factor of 2, with the remaining uncertainty coming from the mass of ^{100}In .

In principle, other uncertainties will also contribute at this level. These include those of masses of lighter Cd isotopes, where similar rp -process branch points occur and which might affect feeding into the ^{99}Cd branch point. In addition, nuclear reaction rate uncertainties will also play a role. However, because reaction rates affect branchings in a linear fashion, while mass differences enter exponentially, mass uncertainties will tend to dominate [26]. Also, which reaction rates are important depends largely on nuclear masses. For example, for low $S_p(^{100}\text{In})$ a (p,γ) - (γ,p) equilibrium will be established between ^{99}Cd and ^{100}In and the $^{100}\text{In}(p,\gamma)$ reaction rate would affect the $A = 99$ production, whereas for larger $S_p(^{100}\text{In})$ the $^{99}\text{Cd}(p,\gamma)$ reaction rate might be more relevant. Therefore, the mass uncertainties should be addressed first. Once they are under control, further improvements might be possible by constraining proton capture rates.

Our results are relevant for any rp -process scenario with a reaction flow through the ^{99}Cd region. Here, we used an x-ray burst model to investigate in detail the impact of our measurements on such an rp process. The νp process in core collapse supernovae might be another possible scenario for an rp process in the ^{99}Cd region. It is planned to also explore whether in that case mass uncertainties have a similar impact on the final composition.

ACKNOWLEDGMENTS

We are grateful to the members of the ISOLDE technical group for their support. We thank V. V. Elomaa and the JYFLTRAP group for providing their data prior to publication. This work was supported by the German Federal Ministry for Education and Research (BMBF) (06GF186I, 06MZ215), the French IN2P3, the EU FP6 Program (MEIF-CT-2006-042114 and EURONS DS Project/515768 RIDS), and the Helmholtz Association for National Research Centers (HGF) (VH-NG-037). H.S. is supported by NSF Grants PHY0606007 and PHY0216783.

-
- [1] K. Blaum, *Phys. Rep.* **425**, 1 (2006).
 - [2] L. Schweikhard and G. Bollen (Eds.), *Int. J. Mass Spectrom.* **251**, (2/3) (2006).
 - [3] M. Mukherjee *et al.*, *Eur. Phys. J. A* **35**, 1 (2008).
 - [4] J. Clark *et al.*, *Nucl. Instrum. Methods B* **204**, 487 (2003).
 - [5] A. Jokinen *et al.*, *Int. J. Mass Spectrom.* **251**, 204 (2006).
 - [6] S. Schwarz *et al.*, *Nucl. Instrum. Methods B* **204**, 507 (2003).
 - [7] M. Block *et al.*, *Eur. Phys. J. A* **25**, s1.49 (2005).
 - [8] J. Dilling *et al.*, *Int. J. Mass Spectrom.* **251**, 198 (2006).
 - [9] B. Franzke, H. Geissel, and G. Münzenberg, *Mass Spectrom. Rev.* **27**, 428 (2008).
 - [10] M. Mukherjee *et al.*, *Phys. Rev. Lett.* **93**, 150801 (2004).
 - [11] M. Mukherjee *et al.*, *Eur. Phys. J. A* **35**, 31 (2008).
 - [12] D. Rodríguez *et al.*, *Phys. Rev. Lett.* **93**, 161104 (2004).
 - [13] D. Rodríguez *et al.*, *Eur. Phys. J. A* **25**, s1.41 (2005).
 - [14] S. Baruah *et al.*, *Phys. Rev. Lett.* **101**, 262501 (2008).
 - [15] P. Delahaye *et al.*, *Phys. Rev. C* **74**, 034331 (2006).
 - [16] G. Sikler *et al.*, *Nucl. Phys.* **A763**, 45 (2005).
 - [17] M. Dworschak *et al.*, *Phys. Rev. Lett.* **100**, 072501 (2008).
 - [18] R. Wallace and S. Woosley, *Astrophys. J. Suppl.* **45**, 389 (1981).
 - [19] H. Schatz *et al.*, *Phys. Rep.* **294**, 167 (1998).
 - [20] C. Fröhlich *et al.*, *Phys. Rev. Lett.* **96**, 142502 (2006).
 - [21] J. Pruet *et al.*, *Astrophys. J.* **644**, 1028 (2006).
 - [22] J. Fallis *et al.*, *Phys. Rev. C* **78**, 022801(R) (2008).
 - [23] K. Lodders, *Astrophys. J.* **591**, 1220 (2003).
 - [24] W. Rapp *et al.*, *Astrophys. J.* **653**, 474 (2006).

- [25] M. Arnould and S. Goriely, *Phys. Rep.* **384**, 1 (2003).
- [26] H. Schatz, *Int. J. Mass Spectrom.* **251**, 293 (2006).
- [27] H. Schatz *et al.*, *Phys. Rev. Lett.* **86**, 3471 (2001).
- [28] S. Gupta *et al.*, *Astrophys. J.* **662**, 1188 (2007).
- [29] N. N. Weinberg, L. Bildsten, and H. Schatz, *Astrophys. J.* **639**, 1018 (2006).
- [30] H. Schatz and K. E. Rehm, *Nucl. Phys.* **A777**, 601 (2006).
- [31] J. L. Fisker, R. D. Hoffman, and J. Pruet, *Astrophys. J. Lett.* **690**, 139 (2009).
- [32] C. Weber *et al.*, *Phys. Rev. C* **78**, 054310 (2008).
- [33] Ch. Weber, K. Blaum, and H. Schatz, *Proc. Sci. NIC X*, 028 (2008).
- [34] E. Kugler, *Hyper. Interact.* **129**, 23 (2000).
- [35] F. Herfurth *et al.*, *Nucl. Instrum. Methods A* **469**, 254 (2001).
- [36] F. Herfurth, *Nucl. Instrum. Methods B* **204**, 587 (2001).
- [37] G. Savard *et al.*, *Phys. Lett.* **A158**, 247 (1991).
- [38] S. Sundell and H. Ravn, *Nucl. Instrum. Methods B* **70**, 160 (1992).
- [39] G. Gräff, H. Kalinowsky, and J. Traut, *Z. Phys. A* **297**, 35 (1980).
- [40] G. Bollen, R. B. Moore, G. Savard, and H. Stolzenberg, *J. Appl. Phys.* **68**, 4355 (1990).
- [41] M. König *et al.*, *Int. J. Mass Spectrom. Ion Process.* **142**, 95 (1995).
- [42] J. Van Roosbroeck *et al.*, *Phys. Rev. Lett.* **92**, 112501 (2004).
- [43] A. Kellerbauer *et al.*, *Eur. Phys. J. D* **22**, 53 (2003).
- [44] C. Guénaut *et al.*, *Phys. Rev. C* **75**, 044303 (2007).
- [45] C. Yazidjian *et al.*, *Phys. Rev. C* **76**, 024308 (2007).
- [46] G. Audi, A. H. Wapstra, and C. Thibault, *Nucl. Phys.* **A729**, 337 (2003).
- [47] A. Martín *et al.*, *Eur. Phys. J. A* **34**, 341 (2007).
- [48] V.-V. Elomaa *et al.*, *Eur. Phys. J. A* **40**, 1 (2009).
- [49] A. H. Wapstra, G. Audi, and C. Thibault, *Nucl. Phys.* **A729**, 129 (2003).
- [50] M. P. Bradley, J. V. Porto, S. Rainville, J. K. Thompson, and D. E. Pritchard, *Phys. Rev. Lett.* **83**, 4510 (1999).
- [51] H. Leutz, K. Schneckenberger, and H. Wennige, *Nucl. Phys.* **63**, 263 (1965).
- [52] W. Goedbloed *et al.*, *Nucl. Instrum. Methods* **88**, 197 (1970).
- [53] M. Nozawa, *Nucl. Phys.* **36**, 411 (1962).
- [54] H. Bakhru, I. M. Ladenbauer-Bellis, and I. Rezanka, *Phys. Rev. C* **3**, 937 (1971).
- [55] R. A. Damerow, R. R. Ries, and W. H. Johnson, *Phys. Rev.* **132**, 1673 (1963).
- [56] E. M. Takagui and O. Dietzsch, *Phys. Rev. C* **21**, 1667 (1980).
- [57] V. R. Bom *et al.*, *Z. Phys. A* **325**, 149 (1986).
- [58] B. W. Filippone, C. N. Davids, R. C. Pardo, and J. Äystö, *Phys. Rev. C* **29**, 2118 (1984).
- [59] N. L. Lark *et al.*, *Nucl. Phys.* **35**, 582 (1962).
- [60] R. Chapman and G. D. Dracoulis, *J. Phys. G* **1**, 657 (1975).
- [61] R. C. Catura and J. R. Richardson, *Nucl. Phys.* **82**, 471 (1966).
- [62] F. A. Johnson, *Can. J. Phys.* **31**, 1136 (1953).
- [63] G. M. Crawley *et al.*, *Phys. Lett.* **B109**, 8 (1982).
- [64] R. A. Dewberry, R. T. Kouzes, and R. A. Naumann, *Phys. Rev. C* **27**, 892 (1983).
- [65] G. Rotbard *et al.*, *Bull. Am. Phys. Soc.* **29**, 1041 (1984).
- [66] V. R. Bom *et al.*, *Z. Phys. A* **331**, 21 (1988).
- [67] M. Karny *et al.*, *GSI Sci. Ref.* **1**, 22 (1998).
- [68] R. C. Pardo, E. Kashy, W. Benenson, and L. W. Robinson, *Phys. Rev. C* **18**, 1249 (1978).
- [69] H. Keller *et al.*, *Z. Phys.* **339**, 355 (1991).
- [70] E. Beck (ISOLDE Collaboration), in *Proceedings of the 2nd International Conference of Nuclei Far from Stability, NUFAST-2 CERN*, 70–30, 1970.
- [71] L. Westgaard *et al.*, in *Proceedings of the 4th International Conference of Atomic Masses and Fundamental Constants*, 1972.
- [72] M. Chartier *et al.*, *Phys. Rev. Lett.* **77**, 2400 (1996).
- [73] K. Rykaczewski *et al.*, *Z. Phys. A* **332**, 275 (1989).
- [74] C. Mazzocchi *et al.*, *Phys. Rev. Lett.* **98**, 212501 (2007).
- [75] R. Cyburt *et al.* (to be published).
- [76] P. Schury *et al.*, *Phys. Rev. C* **75**, 055801 (2007); **80**, 029905(E) (2009).
- [77] A. Kankainen *et al.*, *Phys. Rev. Lett.* **101**, 142503 (2008).